This manuscript is a non-peer reviewed preprint submitted to EarthArXiv.
The corresponding author is Ann Rowan (ann.rowan@uib.no)

Increasing precipitation will offset the impact of warming air temperatures on glacier volume loss in the monsoon-influenced Himalaya until 2100 CE

Anya M. Schlich-Davies[1], Ann V. Rowan[2], Andrew N. Ross[1], Duncan J. Quincey[3], Vivi K. Pedersen[4]

[1]*Priestley International Centre for Climate, School of Earth and Environment, University of Leeds, UK*
[2]*Department of Earth Science, University of Bergen and Bjerknes Centre for Climate Research, Bergen, Norway*
[3]*School of Geography, University of Leeds, UK*
[4]*Department of Geoscience, Aarhus University, Aarhus C, Denmark*

Himalayan glaciers are projected to shrink by over 50% this century due to rising air temperatures. However, the impact of future precipitation change on glacier evolution remains uncertain. Here we explore these precipitation effects by simulating the future evolution of Khumbu Glacier in the monsoon-influenced Himalaya until 2300 CE. Khumbu Glacier is committed by historical warming to volume loss of 23% by 2100 CE. Future warming would increase volume loss up to 70%. We show that moderate warming (RCP4.5) will drive an increase in precipitation that offsets 34% of the potential volume lost due to rising air temperatures. However, extreme warming (RCP8.5) will not be compensated, but will instead drive substantial ablation above 6,000 m, causing the highest glacier on Earth to vanish between 2160 CE and 2260 CE.

Projecting glacier volume change is critical for determining the impact of anthropogenic warming on regional water supplies[1]. However, projections remain challenging because accumulation and ablation in mountain environments is driven by orographic feedbacks between high-relief topography and atmospheric circulation systems such as the South Asian Summer Monsoon[2]. High Mountain Asia is projected to lose 34 ± 19% of glacier ice by 2100 CE if warming is limited to 1.5°C to meet the ambitious Paris Agreement target, equivalent to the most conservative of the IPCC's climate model ensembles (RCP2.6); more realistic future glacier loss is 53 ± 23% under the moderate warming scenario RCP4.5 and 69 ± 20% under the extreme warming scenario RCP8.5[1,3,4]. The assumption underlying global projections that glacier loss is linearly related to increasing air temperature needs consideration in regions with high snowfall. Recent warming resulted in greater precipitation and winter snowfall in the Karakoram and Pamir where glacier mass budgets are balanced or slightly positive[5,6]. A similar effect is suggested, but as yet unexplored, for the monsoon-influenced Himalaya, where changes in the extent and intensity of the Indian Summer Monsoon affected glacier expansion during the Last Glacial Maximum through changes in snowfall[7,8]. Global Climate Models (GCMs) project increasing Indian Summer Monsoon precipitation and variability under global warming[9]. However, as current glacier change projections are forced solely by changes in air temperature, the effects of future changes in the Indian Summer Monsoon and the Westerlies on Himalayan glaciers in terms of precipitation amount, timing and state (i.e., snow/rain) remain poorly understood[10,11].

The challenge of reducing uncertainties in future glacier change projections is complicated by rock debris, which covers 4–7% of glacier surfaces globally[1,12] and 30% of glacier ablation areas in the Himalaya[3]. Satellite observations of glacier mass change across the Himalaya highlighted rates of glacier loss that have accelerated over the last 40 years for both clean-ice glaciers and debris-covered glaciers[13]. However, observations and modelling of individual glaciers show that supraglacial debris significantly affects glacier change over decadal to centennial time scales[14,15]. Ice-dynamical modelling studies assuming clean-ice glaciers in the Everest region projected mass loss greater than 50%[16–18] while similar studies that included the melt-dampening effect of supraglacial debris projected less than 10% mass loss[19] under the same climatic forcing. Debris-covered glaciers are challenging candidates for surface mass balance calculations because ablation is modified by the distribution of supraglacial debris and feedbacks with ice flow[20,21] that promote a longer dynamic response to climatic forcing compared to climatically equivalent clean-ice glaciers[19]. When a glacier is subject to an increasingly negative mass balance, the terminus of the active glacier steps upward in line with the equilibrium line and the lower part of the ablation area is detached and rapidly decays. The process of detachment and decay of the former ablation area is extended in time by the insulation of the ice surface for debris-covered glaciers, where the active terminus initially remains in contact with the stagnant ice mass rather than receding upvalley[15,22,23].

We use novel climate-glacier modelling to simulate the evolution of Khumbu Glacier, Nepal (Fig. 1) from the late Holocene (0 CE) through the present day (2015–2020 CE) until 2300 CE (see Online Methods). To address the significant uncertainties associated with projections of climate change and in particular precipitation change in the monsoon-influenced Himalaya, we use an ensemble approach forced by three Regional Climate Models (RCMs) using multiple time slices that were downscaled using quantile mapping. The RCMs represent a range of possible future climates for the monsoon-influenced Himalaya; the NOAA RCM is characterised by the highest annual precipitation, the IPSL RCM is characterised by the lowest annual precipitation, and the CCCma RCM represents a moderate degree of change. The three downscaled RCMs under two future climate scenarios (RCP4.5 and RCP8.5)[24] are used as inputs to the surface energy and mass balance model COSIPY[25], which includes sublimation in the range of processes that contribute to glacier mass balance, which is an important, but overlooked, contributor to glacier mass loss in the Himalaya[26]. Three present-day and six future clean-ice glacier surface mass balances calculated using COSIPY forced six experiments using the ice-dynamical glacier-evolution model iSOSIA[19,27]. iSOSIA represents the transport of supraglacial debris and feedbacks with mass balance and ice flow, and the accumulation of snow by avalanching that is estimated to provide 75% of glacier mass in this region[15,19]. Local mean annual air temperatures (MAAT) in the Khumbu Valley increase by 1.4 ± 0.4 °C under RCP4.5 and by 3.8 ± 0.2 °C under RCP8.5 by 2100 CE relative to the present day. Greater warming occurs in winter than in summer under both RCPs, as is seen in regional projections[28], resulting in an increase in annual precipitation amount of ~15% with a greater increase in winter compared to summer. As there are no regional temperature projections beyond 2100 CE we used global values; for transient simulations between 2100–2200 CE, a step change in warming relative to 2100 CE was applied to the mass balance for each of the 3 RCMs of 0.5°C for RCP4.5 and 2.8°C for RCP8.5. Transient simulations between 2200–2300 CE used warming of 0.7°C for RCP4.5 and 4.1°C for RCP 8.5 relative to 2100 CE. There are no global projections of precipitation change or of the other climate parameters used beyond 2100 CE so no precipitation change was applied after 2100 CE (See Supplementary material).

Results

Present-day glacier mass balance and dynamics

Between the three RCMs the mass balance calculated in the NOAA experiment gives the best fit to observations in terms of annual total precipitation, inter-annual precipitation and air temperature. The simulation forced using the NOAA RCM gave the best fit to observations of current glacier extent, dynamics and recent mass change and is therefore used as the starting point for the simulations of future glacier evolution using each of the three RCM forcings under two RCPs (Fig. 2). In considering the present state of Khumbu Glacier, we simulate the active glacier and assign the former debris-covered tongue to the model domain as a topographic feature[15,29–31]. The glacier extent and mass balance are underestimated if supraglacial debris and avalanching are not simulated. Across the three present-day simulations, mass balance calculated using the NOAA RCM is more positive than that resulting from the ISPL and CCCma RCMs and gives the best fit to observations of air temperature and precipitation in terms of the annual total, seasonality and variability. Simulated glacier area is 7.8 km^2, similar to structural mapping observations of the active glacier[30]. Simulated ice thickness at the terminus is 130 m, similar to a geophysical survey[32]. Simulated ice-surface elevation change in the lower ablation area is –30 m over 20 years, similar to satellite observations for 1984–2015 CE[14]. Simulated velocities reach a maximum of 220 m a^{-1} and match closely with remote sensing observations[33] (Fig. 3).

Climate change and glacier evolution from present day until 2100 CE

Khumbu Glacier is responding to historical climatic forcing and will shrink even if warming ceases today. Indeed, according to our equilibrium simulation from the NOAA experiment, the active terminus will recede by 2.1 km and the maximum ice thickness will decrease from 246 m to 206 m (40 m) by 2100 CE without additional warming (Fig. 3). Supraglacial debris up to 1.3 m thick extending 1 km up-glacier from the terminus sustains ~10% more ice volume than would be the case for a clean-ice surface. The rate of ice volume loss is highest from the present day until 2070 CE when, in the absence of any further climate warming, the glacier approaches equilibrium with the historical forcing such that the committed ice volume loss is 23% by 2100 CE (Fig. 4).

In the NOAA RCP4.5 experiment, glacier volume decreases by 36% between the present day and 2100 CE (Fig. 4). While significant, this end-of-century mass loss is partially offset by an increase in precipitation compared to the CCCma RCP4.5 experiment with volume loss of 57% owing to a much smaller increase in precipitation. An equivalent simulation forced only by warming of 1.4°C resulted in 70% volume loss, demonstrating that up to 34% of potential future glacier loss is compensated by the changes in precipitation that result from warming air temperatures. Specifically, in the NOAA RCP4.5 experiment, MAAT warms by 1.4°C by 2100 CE to reach –0.75°C, and is similar in summer and winter, resulting in an increase in precipitation amount of 15% (from 581 mm to 665 mm) with the largest change occurring in winter. As a result, the spatially averaged cumulative mass balance is –0.14 m water equivalent (w.e.) a^{-1} in 2100 CE and slightly lower from the present-day value of –0.21 m w.e. a^{-1}. Therefore, keeping warming within the limits of RCP4.5 would cause limited further decay of Khumbu Glacier from that already committed to by historical warming. For the NOAA RCP8.5 climate forcing, MAAT warms by 3.8°C by 2100 CE and the increase in annual precipitation of 15% is not sufficient to offset glacier loss resulting from this extreme warming (Fig. 4).

The mean glacier volume loss by 2100 CE across the RCM ensemble under RCP4.5 is 0.399 $\times 10^9$ km^3 (46% of present-day volume) and 0.506 $\times 10^9$ km^3 (57%) under RCP8.5. The CCCma experiment has a 1% difference in volume loss between RCP4.5 and RCP8.5 despite a 1.9°C difference in MAAT. This surprising result, given the significant temperature difference, can be accounted for by a higher number of high-magnitude precipitation events under RCP8.5 in combination with a small difference in winter temperatures between the two RCPs; maximum winter temperature is 1.7°C higher for CCCma than for the other RCMs under RCP4.5, thus allowing the occurrence of some ablation and rainfall during the winter. Under RCP8.5 all ensemble simulations gave similar results for mass balance and ice volume, with only a 10% difference in final glacier volume between RCMs.

Climate change and glacier evolution from 2100 CE until 2300 CE

Until now we simulated Khumbu Glacier in equilibrium with the projected end-of-century climate to investigate a scenario where climate change mitigation measures would prevent further warming beyond 2100 CE. Indeed, if climate conditions in 2100 CE and beyond are limited to the RCP4.5 scenario, then Khumbu Glacier will recede to the base of the icefall with insignificant change in ice volume after 2100 CE (Fig. 4). Projections of climate change beyond 2100 CE are more uncertain than those for this century but do give rise to a clear prognosis for the future of Khumbu Glacier. In every experiment under RCP4.5 (increase in MAAT of 0.7°C between 2100 CE and 2300 CE) there is little change in glacier volume between 2200 CE and 2300 CE regardless of the RCM forcing used. In the NOAA RCP4.5 experiment, the icefall is maintained such that ice continues to flow below 6,000 m and the glacier can remain in contact with the dynamically detached stagnant tongue. These results demonstrate that Khumbu glacier can reach a new dynamic equilibrium under RCP4.5 that maintains a sufficient ice thickness to protect against catastrophic mass loss for at least two centuries.

Every experiment under RCP8.5 (increase in MAAT of 4.1°C between 2100 CE and 2300 CE) results in substantial glacier loss after 2100 CE, and the demise of Khumbu Glacier before 2300 CE regardless of the RCM used (Fig. 4b). Physical detachment of the debris-covered tongue from the active glacier, whereby ice no longer occupies the area at the base of the icefall, occurs around 2070 CE in the CCCma and IPSL experiments and around 2140 CE in the NOAA experiment (Fig. 3). Khumbu Glacier is no longer considered a viable glacier system when only a small ice volume with negligible flow (<10 m a^{-1}) remains within the former glacier extent. In the NOAA RCP8.5 experiment, the glacier area is only 1.2 km^2 and the mean surface velocity reduces to 10 m a^{-1} in 2260 CE, such that the glacier is no longer considered viable after this time. Glacier breakdown occurs earlier for the CCCma and IPSL RCMs where mass loss is not compensated for by an increase in precipitation of the same magnitude as that projected by the NOAA RCM.

Discussion

Projections of glacier change and sustainability require consideration of the meteorological and glaciological processes that interact to drive the surface change and redistribution of glacier mass. The majority of glaciers in the Himalaya are located above 5,000 m, but despite their high elevations these glaciers are undergoing rapid loss of ice in response to anthropogenic climate change[13]. Our projections of volume change for Khumbu Glacier show high variability between RCMs resulting from differences in projected precipitation change and variability. Our results show that the mass balance of Khumbu Glacier is close to zero under RCP4.5, particularly after 2200 CE, suggesting that the future of monsoon-influenced Himalayan glaciers can be secured by reducing the magnitude of projected anthropogenic climate change. Contrary to previous studies that only considered the impact of air temperature on glacier change[1,16,18], our results take into account the committed glacier volume loss in the monsoon-influenced Himalaya of 23% by 2100 CE, and show that the projected increase in annual precipitation amount under RCP4.5 is sufficient to offset half of glacier loss that would result from 1.4°C of warming, thus limiting the total glacier volume lost to 36%. Therefore, if global efforts are sufficient to mitigate further warming after 2100 CE in line with RCP4.5, then high-elevation Himalayan glaciers can persist until 2300 CE and potentially further into the future.

To address the uncertainties associated with projections of precipitation change in the monsoon-influenced Himalaya, we used an ensemble approach with three RCMs and two RCPs to explore possible future variability in precipitation in this region. The experimental design used here represents an advance compared with previous glacier modelling efforts in this region through the robust representation of distributed mass balance including snow avalanching and sublimation processes and the feedbacks between supraglacial debris transport, mass balance and ice flow. Particularly, the distributed mass balance forcing and the evolution of the supraglacial debris feedback are important for driving recent and future glacier evolution. In addition, previous studies have not accounted for the committed glacier response to historical warming when estimating glacier mass balance changes[1,16] or considered that the most recent expansion of glaciers during the Little Ice Age around 500 years ago was not a dynamically stable or spatially consistent event[34]. Our simulations represent a robust approach to quantify the present-day imbalance for Himalayan glaciers as they start from the late Holocene and consider the long-term dynamic response of glaciers to climate change. Such an approach may not be needed to project glacier change into future centuries. Our results show that the relationship between response time and mass balance is insignificant after 2100 CE when Khumbu Glacier is so small that dynamic behaviour had little impact on mass change (see Supplementary material).

While we have considered the effects on glacier surface mass balance of mesoscale-scale meteorological variables, smaller scale processes operating close to the ice surface also affect mass balance. Observations from an automatic weather station on Khumbu Glacier (6,464 m) indicate that surface energy fluxes may be sufficient to cause non-negligible melting of glacier surfaces despite freezing air temperatures[35]. In addition, katabatic winds are suggested to explain a local 15-year decrease in maximum air temperature and precipitation over glaciers in the Himalaya while minimum air temperatures continue to rise[36]. However, the impact of micro-scale near-surface cooling on the duration and extent of mesoscale-scale precipitation and therefore glacier mass balance is likely to be minimal. Results from an ice core from South Col Glacier combined with COSIPY suggested that ablation may take place even at the highest elevations (>8,000 m) in the Himalaya[37]. However, a similar study of South Col Glacier demonstrated the large uncertainties associated with simulating surface mass balance at such high elevations where sub-daily air temperature gradients and the duration of snow cover are important controls on ablation and accumulation[38]. Our results show that glacier surface mass balance calculations also require consideration of meteorological patterns and trends tot account for the large uncertainties associated with projections of changes in monsoon precipitation[10,11,38,39].

Current global greenhouse emissions are following the trajectory of the moderate warming scenario RCP4.5, and the extreme warming scenario RCP8.5 should be described as 'low-possibility, high-impact'[40]. Mountain regions are warming more rapidly than global mean[41] such that a global temperature rise of 1.5°C will lead to 2.1 ± 0.1°C of warming in High Mountain Asia[3,41], although the occurrence of elevation-dependent warming above 5,000 m is debated[42]. Therefore, it is possible that future glacier change in the monsoon-influenced Himalaya may follow a trajectory that is closer to RCP8.5 than RCP4.5. Under RCP4.5, Khumbu Glacier has a similar extent in 2100 CE to the active section of the present-day glacier, rather than the extent mapped in global inventories that include the dynamically detached debris-covered tongue[15]. However, a similar stabilisation in glacier volume will not occur under RCP8.5 as warming of 3.8°C by 2100 CE will significantly increase ablation, even at the highest elevations, regardless of any accompanying increase in precipitation. We found no evidence of future increases in precipitation offsetting RCP8.5 warming over the next 80 years; net glacier mass balance was strongly negative in all experiments. High-magnitude precipitation events from winter Westerly disturbances increased by up to a factor of seven between the present day and 2100 CE under RCP8.5 and could make the net annual mass balance less negative than would be the case when solely forced by change in MAAT. Under RCP8.5, glacier mass balance in the monsoon-influenced Himalaya may therefore shift from being driven by accumulation during the monsoon season to predominantly winter accumulation, with monsoon precipitation resulting in mass gain at only the very highest elevations. This outcome can be avoided by limiting anthropogenic warming to within the RCP4.5 scenario, which, due to the associated increase in precipitation will protect 60% of the current glacier volume until at least 2100 CE.

Online Methods

Regional climate model (RCM) downscaling

Daily data from the Coordinated Regional Downscaling Experiment (CORDEX) South Asia domain were downloaded from the Indian Institute of Tropical Meteorology website (http://cccr-dx.tropmet.res.in:8000/cccrindia/) for the grid box nearest to Khumbu Glacier (27.9065°N, 86.4353°E). Incoming shortwave and longwave radiation components were downloaded from the ESGF portal (https://esgf-index1.ceda.ac.uk/search/cordex-ceda/). Three RCMs were chosen to span the range of possible precipitation future scenarios and subject to quantile mapping in order to force separate glacier mass balance calculations. Observational data from automatic weather stations collected between January 2006 and November 2019 by Ev-K2-CNR and GlacioClim (https://glacioclim.osug.fr/) were used to aid RCM downscaling with gaps filled with interpolated data from neighbouring stations where possible. The automatic weather station data were used to disaggregate daily downscaled present-day and end-of-century climate data to an hourly resolution[43] using seasonal means to reproduce the 'nocturnal peak' seen during the monsoon. The MELODIST Python tool was used for all other meteorological variables[44]. The climate time-slice for the period 2095–2100 CE was used to force the future mass balance simulations and drive the ice-flow model from the present-day simulation. Time-slices representing five-year periods were chosen to reduce the computational expense of the glacier modelling, though the preceding decade was also used for comparison with the time-slice climate data. The climate forcing for the downscaled NOAA RCM under RCP 4.5 was 1.4°C higher than present day (MAAT of –0.75°C in 2095–2100 CE compared with –2.15°C in 2015–2020 CE). Annual precipitation increased by 14.8% from 581.4 mm in the present day to 664.8 mm a^{-1} in 2100 CE under RCP4.5, of which summer (JJAS) precipitation increased by 5.4% and winter (DJF) precipitation increased by 14.1%. The climate forcing for the downscaled NOAA RCM under RCP 8.5 was 3.8°C higher than present day (MAAT of 1.65°C in 2095–2100 CE). Annual precipitation increased by 14.9% in 2100 CE under RCP8.5, of which summer precipitation increased by 9.8% and winter precipitation increased by 19.4%.

Surface energy and mass balance modelling using COSIPY

The Coupled Snowpack and Ice-surface Energy and Mass Balance model in Python (COSIPY) is an open-source distributed surface energy balance model[25]. The model is developed and modularised in Python and has been applied to a range of mountain glaciers including those in High Mountain Asia[38,45]. COSIPY integrates a surface energy balance model with a multi-layer snow and ice model and thereby resolves all energy fluxes at the ice surface that contribute to surface melt. COSIPY includes a calculation of sublimation, which is an important ablation process for high-elevation glaciers in the Himalaya[20]. A 30-m digital elevation model was acquired from the Shuttle Radar Topography Mission[46] and resampled to 100-m grid spacing. The topographic rather than subglacial surface was used to calculate surface mass balance. Each experiment was forced using a 100 m grid of annual clean-ice glacier mass balance. COSIPY calculates clean-ice mass balance and does not parameterise snow avalanching meaning the impact of supraglacial debris on ablation rates and avalanching on accumulation rates was handled subsequently by the glacier model iSOSIA.

Glacier evolution modelling using iSOSIA

The integrated second-order shallow ice approximation model (iSOSIA) is a 3-D depth-integrated, higher-order ice-dynamical glacier-evolution model that solves for the flow of ice, including the influence of longitudinal and transverse stress gradients that are imposed on ice flow through high-relief topography[27]. The model was originally used to study glacial landscape evolution and has been developed for simulation of debris-covered glaciers by incorporating the feedbacks between debris transport, mass balance and ice flow[19]. Estimates of distributed ice thickness[47] were subtracted from the 30-m digital elevation model to yield an estimate of the subglacial topography that was used as the glacier model domain. The ice-free model domain incorporates the full hydrological catchment and includes the steep hillslopes of the Western Cwm that provide snow to the glacier's accumulation area. The domain comprises 19,164 glacier points in a square grid and provided the basis for both the mass balance and ice flow simulations.

The glacier model parameterisation and experimental design followed that used in our previous work[15]. For glaciers in the Himalaya, 75% of accumulation is estimated to occur by snow avalanching rather than direct snowfall[48]. In the model, snow avalanching was represented by removing snow and ice from hillslopes with a slope greater than 28° and distributing using a non-linear hillslope flux model[49] across the ice surface. This avalanching routine was previously applied to Khumbu Glacier and found to be sufficient to prevent snow and ice accumulation on slopes that are observed to be bare whilst allowing accumulation on steep sections of the glacier. Debris is delivered to the glacier surface from headwalls using a similar non-linear hillslope flux model as the avalanching routine and debris concentrations from hillslopes without ice assumed a mean erosion rate of 1 mm a^{-1}. The reduction in ablation from clean-ice values beneath continuous supraglacial debris is represented as a reciprocal function that scales clean-ice ablation (b_{clean}) to give sub-debris melt rates (b_{debris}) as a function of debris thickness (h):

$$b_{debris} = b_{clean} \times \frac{h_0}{h + h_0} \qquad \text{Eq(1)}$$

where h_0 is a constant representing the characteristic debris thickness at which the reduction in ablation due to insulation by supraglacial debris is 50% of the value for an equivalent clean-ice surface. The value for h_0 of 0.8 m represents a positively skewed supraglacial debris thickness distribution that includes ablation 'hotspots' such as supraglacial ponds and ice cliffs that is representative of the current state of Khumbu Glacier[15]. Observations and modelling of the dynamics and structure of Khumbu Glacier show that the lower 5 km (25% of the total length, 20% of total ice volume) is stagnant and dynamically detached from the active glacier in the last 100 years[15,23]. Basal ice at the glacier surface indicates that the active terminus overrides the stagnant tongue[29] and surface displacement measurements indicate that ice no longer flows longitudinally through the detached debris-covered tongue and is instead collapsing laterally at 3 m a^{-1},[31]. The simulated active glacier matches observed changes in the spatial distribution of surface debris[30] and feature-tracking and remote-sensing observations of surface elevation change[14]. We therefore simulate the active glacier and assign the former debris-covered tongue to the model domain as a static topographic feature.

Figures and captions

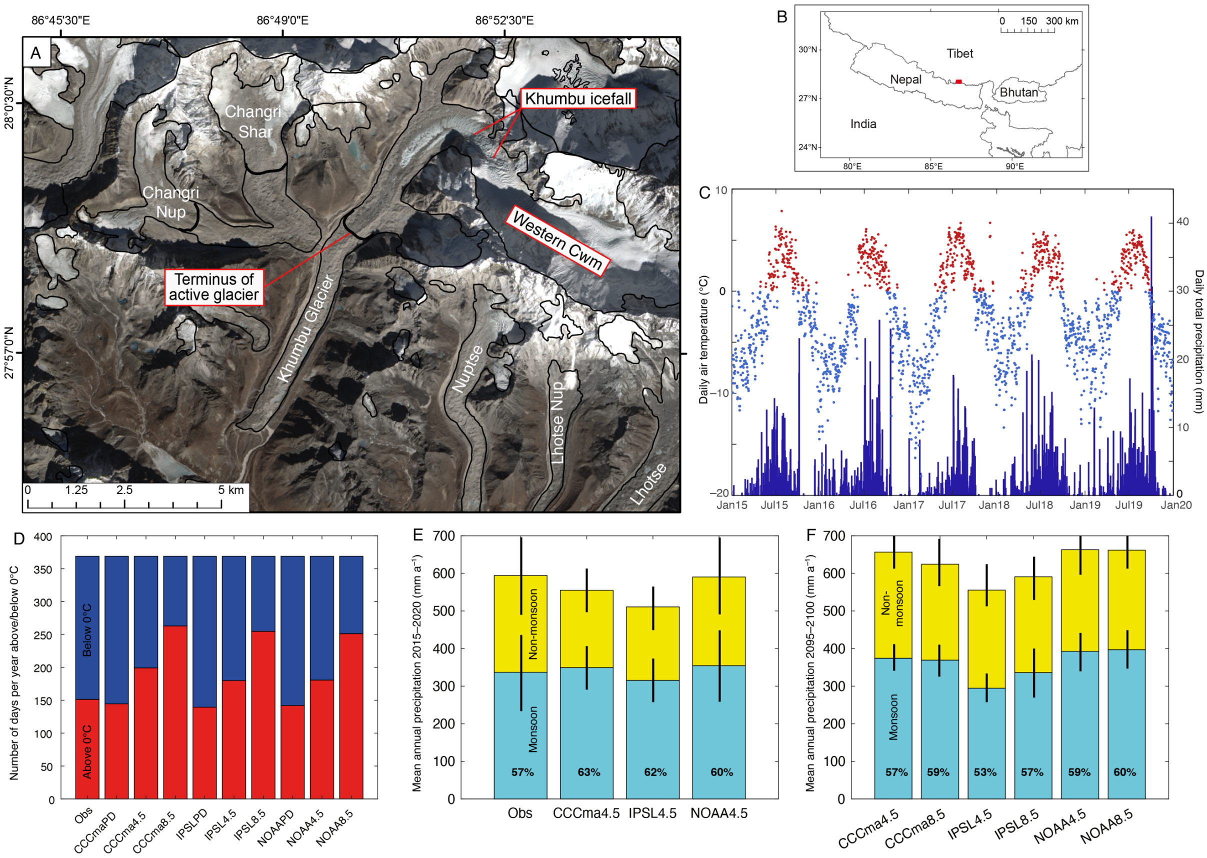

Figure 1: Khumbu Glacier location, climate data and downscaled regional climate model results. (a) Satellite image of glaciers in the Khumbu Valley showing the extent of supraglacial debris, locations of the icefall and the extent of active ice flow inferred from observations of glacier velocity (black lines). (b) regional location of (a). (c) Daily mean temperature and daily total precipitation from the NOAA regional climate model (RCM) for the present day (2015–2020 CE) following downscaling using quantile mapping with air temperature categorised into above freezing (red) and below freezing (blue). (d) Proportion of air temperatures above and below freezing for the present day for each RCM and RCP for the downscaled daily data compared with observations. (e) Annual precipitation totals for non-monsoon and monsoon with standard deviation between selected years shown by black bars for the downscaled daily data compared with observations. (f) Future (2095–2100 CE) time-slice annual precipitation totals for non-monsoon and monsoon months with standard deviation between selected years shown by black bars. In (e) and (f) the percentage of the total annual precipitation occurring during the monsoon is indicated by the value in bold text.

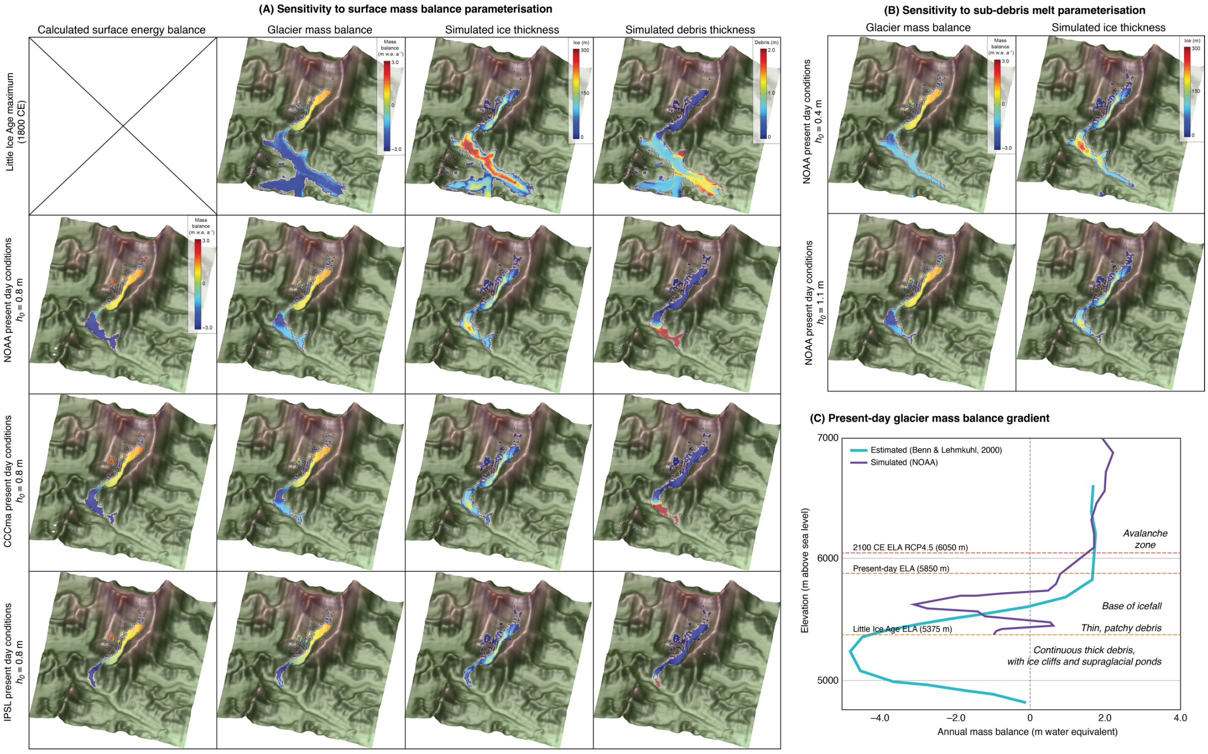

Figure 2. Glacier model sensitivity to the surface energy and mass balance forcing and sub-debris melt parameterisation for the simulations of the active section of Khumbu Glacier. (a) Little Ice Age glacier mass balance, ice thickness and debris thickness. Surface mass balance calculated using COSIPY forced by the downscaled Regional Climate Model outputs, glacier mass balance calculated using the same climate forcing following integration with iSOSIA to represent the impact of differential ablation beneath supraglacial debris (h_0 of 0.8 m) simulated ice thickness and debris thickness resulting from each forcing. (b) glacier mass balance calculated using the NOAA climate forcing and the resulting simulated ice thickness for alternative h_0 values of 0.4 m and 1.1 m. (c) Estimated mass balance gradient for debris-covered glaciers in the Everest region[48] compared with the glacier mass balance gradient simulated using the NOAA climate forcing and a value for h_0 of 0.8 m, with the equilibrium line altitude (ELA) at different points in the historical and future (NOAA RCP4.5) experiments.

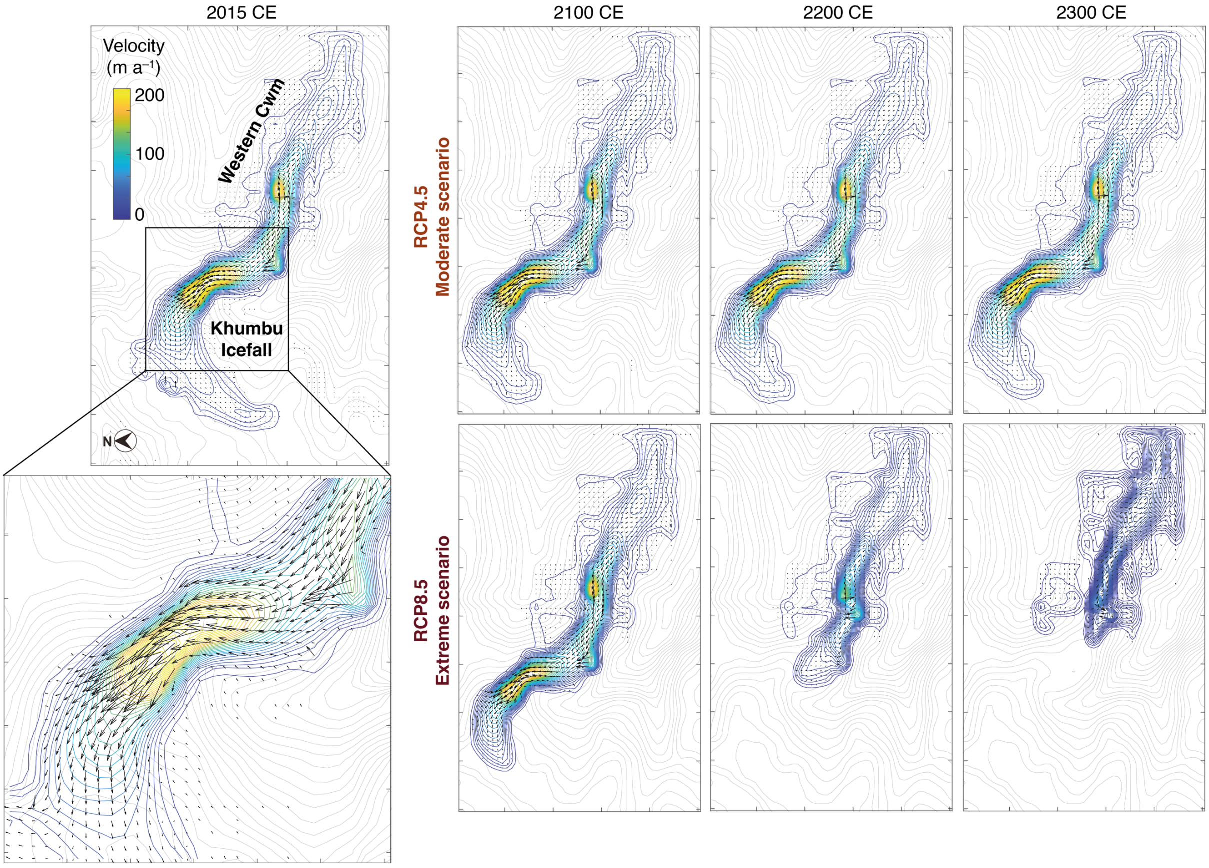

Figure 3. Simulated ice flow for Khumbu Glacier. Velocity-vector maps showing simulated ice flow magnitude and direction from the present day (2015–2020 CE) until 2300 CE under RCP4.5 (moderate warming) and RCP8.5 (extreme warming) using the downscaled NOAA climate forcing and a value for h_0 of 0.8 m. Simulated ice flow speed is shown as colour shading with blue contours, and the bed topography is shown by coloured contours. For the present day, the simulated ice flow is shown in detail for the Khumbu icefall and compared with measurements of glacier surface speed[33]. Note that rapid flow across the Western Cwm indicated by one arrow shows the effects of avalanching rather than sustained glacier flow.

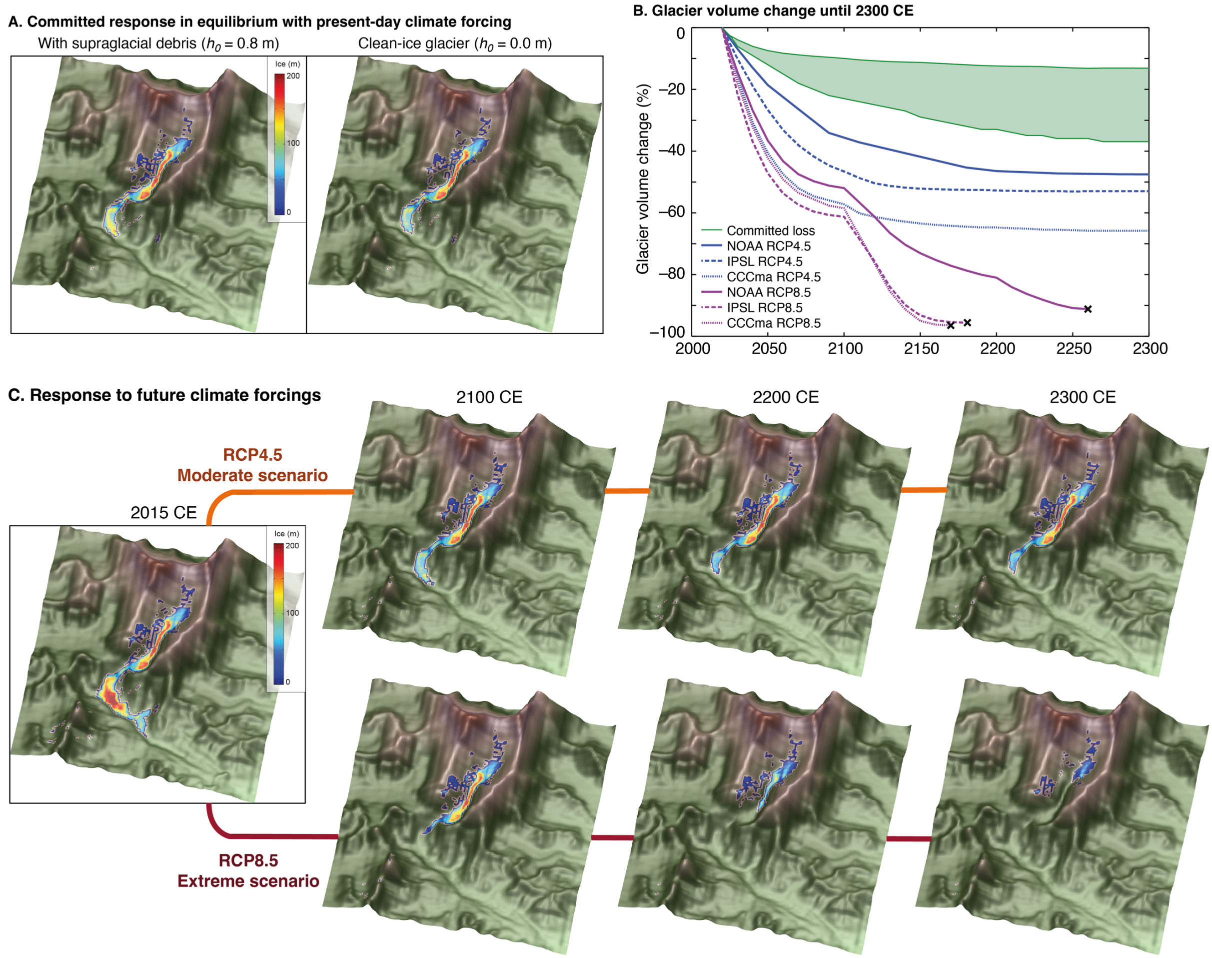

Figure 4. Future glacier volume change projections. (a) Equilibrium ice thickness accounting for the committed response to recent climate change using the downscaled NOAA climate forcing where the glacier is in dynamic equilibrium with the present-day climate, with and without the effect of sub-debris melt. (b) Simulated glacier volume change from the present day (2015–2020 CE) until 2300 CE under RCP4.5 (moderate warming) and RCP8.5 (extreme warming) for the three downscaled RCM forcings. The black crosses mark when ice flow has declined sufficiently that the glacier is considered almost absent or no longer viable. The green shading shows the range of the committed loss, accounting for the effect of supraglacial debris on glacier change, (c) Simulated ice thickness for 2100 CE, 2200 CE and 2300 CE using the downscaled NOAA climate forcing and a value for h_0 of 0.8 m.

References

1. Rounce, D. R. *et al.* Global glacier change in the 21st century: Every increase in temperature matters. *Science* **379**, 78–83 (2023).
2. Bookhagen, B. & Burbank, D. W. Topography, relief, and TRMM-derived rainfall variations along the Himalaya. *Geophys. Res. Lett.* **33**, L08405 (2006).
3. Kraaijenbrink, P. D. A., Bierkens, M. F. P., Lutz, A. F. & Immerzeel, W. W. Impact of a global temperature rise of 1.5 degrees Celsius on Asia's glaciers. *Nature* **549**, 257–260 (2017).
4. Marzeion, B. *et al.* Partitioning the Uncertainty of Ensemble Projections of Global Glacier Mass Change. *Earth's Future* **8**, e2019EF001470 (2020).
5. Dehecq, A. *et al.* Twenty-first century glacier slowdown driven by mass loss in High Mountain Asia. *Nature Geosci* **12**, 22–27 (2019).
6. Farinotti, D., Immerzeel, W. W., de Kok, R. J., Quincey, D. J. & Dehecq, A. Manifestations and mechanisms of the Karakoram glacier Anomaly. *Nat. Geosci.* **13**, 8–16 (2020).
7. Benn, D. I. & Owen, L. A. The role of the Indian summer monsoon and the mid-latitude westerlies in Himalayan glaciation: review and speculative discussion. *Journal of the Geological Society* **155**, 353–363 (1998).
8. Owen, L. A. *et al.* Quaternary glaciation of Mount Everest. *Quaternary Science Reviews* **28**, 1412–1433 (2009).
9. Katzenberger, A., Schewe, J., Pongratz, J. & Levermann, A. Robust increase of Indian monsoon rainfall and its variability under future warming in CMIP6 models. *Earth Syst. Dynam.* **12**, 367–386 (2021).
10. Mölg, T., Maussion, F. & Scherer, D. Mid-latitude westerlies as a driver of glacier variability in monsoonal High Asia. *Nature Clim Change* **4**, 68–73 (2014).
11. Shaw, T. E. *et al.* Multi-decadal monsoon characteristics and glacier response in High Mountain Asia. *Environ. Res. Lett.* **17**, 104001 (2022).
12. Herreid, S. & Pellicciotti, F. The state of rock debris covering Earth's glaciers. *Nat. Geosci.* **13**, 621–627 (2020).
13. Maurer, J. M., Schaefer, J. M., Rupper, S. & Corley, A. Acceleration of ice loss across the Himalayas over the past 40 years. *Sci. Adv.* **5**, eaav7266 (2019).
14. King, O. *et al.* Six Decades of Glacier Mass Changes around Mt. Everest Are Revealed by Historical and Contemporary Images. *One Earth* **3**, 608–620 (2020).
15. Rowan, A. V. *et al.* The Role of Differential Ablation and Dynamic Detachment in Driving Accelerating Mass Loss From a Debris-Covered Himalayan Glacier. *J. Geophys. Res. Earth Surf.* **126**, (2021).
16. Shea, J. M., Immerzeel, W. W., Wagnon, P., Vincent, C. & Bajracharya, S. Modelling glacier change in the Everest region, Nepal Himalaya. *The Cryosphere* **9**, 1105–1128 (2015).
17. Soncini, A. *et al.* Future hydrological regimes and glacier cover in the Everest region: The case study of the upper Dudh Koshi basin. *Science of The Total Environment* **565**, 1084–1101 (2016).
18. Zhang, T. *et al.* Projections of Peak Water Timing From the East Rongbuk Glacier, Mt. Everest, Using a Higher-Order Ice Flow Model. *Earth's Future* **12**, e2024EF004545 (2024).
19. Rowan, A. V., Egholm, D. L., Quincey, D. J. & Glasser, N. F. Modelling the feedbacks between mass balance, ice flow and debris transport to predict the response to climate change of debris-covered glaciers in the Himalaya. *Earth and Planetary Science Letters* **430**, 427–438 (2015).
20. Bonekamp, P. N. J., Wanders, N., Wiel, K., Lutz, A. F. & Immerzeel, W. W. Using large ensemble modelling to derive future changes in mountain specific climate indicators in a 2 and 3°C warmer world in High Mountain Asia. *Int J Climatol* **41**, (2021).
21. Nicholson, L. & Benn, D. I. Properties of natural supraglacial debris in relation to modelling sub-debris ice ablation: *Earth Surf. Process. Landforms* **38**, 490–501 (2013).
22. Pellicciotti, F. *et al.* Mass-balance changes of the debris-covered glaciers in the Langtang Himal, Nepal, from 1974 to 1999. *J. Glaciol.* **61**, 373–386 (2015).
23. Quincey, D. J., Luckman, A. & Benn, D. Quantification of Everest region glacier velocities between 1992 and 2002, using satellite radar interferometry and feature tracking. *J. Glaciol.* **55**, 596–606 (2009).
24. Collins, M., Knutti, R., & Arblaster, J. Long-term Climate Change: Projections, Commitments and Irreversibility. In: Climate Change 2013: The Physical Science Basis. Contribution of Working

Group I to the Fifth Assessment Report of the Intergovernmental Panel on Climate Change [Stocker, T.F., D. Qin, G.-K. Plattner, M. Tignor, S.K. Allen, J. Boschung, A. Nauels, Y. Xia, V. Bex and P.M. Midgley (eds.)]. Cambridge University Press, Cambridge, United Kingdom and New York, NY, USA,, 1–108. (2013).

25. Sauter, T., Arndt, A. & Schneider, C. COSIPY v1.3 – an open-source coupled snowpack and ice surface energy and mass balance model. *Geosci. Model Dev.* **13**, 5645–5662 (2020).
26. Stigter, E. E. *et al.* The Importance of Snow Sublimation on a Himalayan Glacier. *Front. Earth Sci.* **6**, 108 (2018).
27. Egholm, D. L., Knudsen, M. F., Clark, C. D. & Lesemann, J. E. Modeling the flow of glaciers in steep terrains: The integrated second-order shallow ice approximation (iSOSIA). *J. Geophys. Res.* **116**, (2011).
28. Sanjay, J., Krishnan, R., Shrestha, A. B., Rajbhandari, R. & Ren, G.-Y. Downscaled climate change projections for the Hindu Kush Himalayan region using CORDEX South Asia regional climate models. *Advances in Climate Change Research* **8**, 185–198 (2017).
29. Miles, K. E. *et al.* Continuous borehole optical televiewing reveals variable englacial debris concentrations at Khumbu Glacier, Nepal. *Commun Earth Environ* **2**, 12 (2021).
30. Nakawo, M. Processes which distribute supraglacial debris on the khumbu glacier, nepal himalaya. *Ann. Glaciol.* **8** 129–131 (1986).
31. Watson, C. S. *et al.* Quantifying ice cliff evolution with multi-temporal point clouds on the debris-covered Khumbu Glacier, Nepal. *J. Glaciol.* **63**, 823–837 (2017).
32. Gades, A., Conway, H., Nereson, N., Naito, N. & Kadota, T. Radio echo-sounding through supraglacial debris on Lirung and Khumbu Glaciers, Nepal Himalayas. *Debris-Covered Glaciers (Proceedings of a workshop held at Seattle, Washington, USA, September 2000). IAHS* **264**, 13–22 (2000).
33. Altena, B. & Kääb, A. Ensemble matching of repeat satellite images applied to measure fast-changing ice flow, verified with mountain climber trajectories on Khumbu icefall, Mount Everest. *J. Glaciol.* **66**, 905–915 (2020).
34. Lee, E. *et al.* Accelerated mass loss of Himalayan glaciers since the Little Ice Age. *Sci Rep* **11**, 24284 (2021).
35. Matthews, T. *et al.* Going to Extremes: Installing the World's Highest Weather Stations on Mount Everest. *Bulletin of the American Meteorological Society* **101**, E1870–E1890 (2020).
36. Salerno, F. *et al.* Local cooling and drying induced by Himalayan glaciers under global warming. *Nat. Geosci.* **16**, 1120–1127 (2023).
37. Potocki, M. *et al.* Mt. Everest's highest glacier is a sentinel for accelerating ice loss. *npj Clim Atmos Sci* **5**, 7 (2022).
38. Brun, F. *et al.* Everest South Col Glacier did not thin during the period 1984–2017. *The Cryosphere* **17**, 3251–3268 (2023).
39. Khadka, A. *et al.* Weather on MOUNT EVEREST during the 2019 summer MONSOON. *Weather* **76**, 205–207 (2021).
40. Pedersen, J. S. T. *et al.* Variability in historical emissions trends suggests a need for a wide range of global scenarios and regional analyses. *Commun Earth Environ* **1**, 41 (2020).
41. Pepin, N. C. *et al.* Climate Changes and Their Elevational Patterns in the Mountains of the World. *Reviews of Geophysics* **60**, (2022).
42. Gao, Y. *et al.* Does elevation-dependent warming hold true above 5000 m elevation? Lessons from the Tibetan Plateau. *npj Clim Atmos Sci* **1**, 19 (2018).
43. Debele, B., Srinivasan, R. & Yves Parlange, J. Accuracy evaluation of weather data generation and disaggregation methods at finer timescales. *Advances in Water Resources* **30**, 1286–1300 (2007).
44. Förster, K., Hanzer, F., Winter, B., Marke, T. & Strasser, U. An open-source MEteoroLOgical observation time series DISaggregation Tool (MELODIST v0.1.1). *Geosci. Model Dev.* **9**, 2315–2333 (2016).
45. Huintjes, E., Neckel, N., Hochschild, V. & Schneider, C. Surface energy and mass balance at Purogangri ice cap, central Tibetan Plateau, 2001–2011. *J. Glaciol.* **61**, 1048–1060 (2015).
46. Farr, T. G. *et al.* The Shuttle Radar Topography Mission. *Reviews of Geophysics* **45**, 2005RG000183 (2007).

47. Farinotti, D. *et al.* A consensus estimate for the ice thickness distribution of all glaciers on Earth. *Nat. Geosci.* **12**, 168–173 (2019).
48. Benn, D. I. & Lehmkuhl, F. Mass balance and equilibrium-line altitudes of glaciers in high-mountain environments. *Quaternary International* **65–66**, 15–29 (2000).
49. Roering, J. J., Kirchner, J. W. & Dietrich, W. E. Evidence for nonlinear, diffusive sediment transport on hillslopes and implications for landscape morphology. *Water Resources Research* **35**, 853–870 (1999).

Acknowledgements
ASD was also supported by the Priestley International Centre for Climate at the University of Leeds, and a University of Leeds Anniversary Research Scholarship. AVR was supported by a Royal Society Dorothy Hodgkin Research Fellowship (DHF\R1\201113). We thank Tobias Sauter and Anselm Arndt for developing and sharing COSIPY with the glaciology community and for helping ASD with questions about the model. Thanks to Patrick Wagnon for sharing the Pyramid and Changri Nup Glacier automatic weather station data.

Supplementary material to: **Increasing precipitation will offset the impact of warming air temperatures on glacier volume loss in the monsoon-influenced Himalaya until 2100 CE**

1. Regional Climate Model forcing of glacier mass balance

This study used three Regional Climate Models (RCMs) from the CORDEX project that have been dynamically downscaled from CMIP5 coarse GCM data by the Indian Institute of Tropical Meteorology to a 50 km spatial resolution (Lutz et al., 2016). CORDEX daily climate data were downloaded from this website for the grid box nearest to Khumbu Glacier (27.9065056°N, 86.4352951°E), representing the Dudh Koshi at ~2,100 m a.s.l. These data include the climate variables used to force the COSIPY mass balance model (temperature, precipitation, the radiation components, wind speed, relative humidity and atmospheric pressure). A single RCM was not considered sufficient for representing both present-day climate and potential future climatic extremes. A multi-model mean approach, which is widely used elsewhere, was also not considered sufficient to represent present-day and future climate conditions in the Khumbu Valley, as this approach gives equal weighting to models with poor and good performance in their ability to reproduce climate (Pierce et al., 2009). RCMs were assessed on their fidelity to present-day climate, also known as hindcasting (Biemans et al., 2013), with emphasis on temperature seasonality and seasonal precipitation dynamics, given the importance of these variables for glacier mass balance. Three RCMs representing discrete precipitation scenarios were selected (Table S1); referred to here as NOAA, CCCma, and IPSL, to represent either wet, moderate and dry climates in 2080–2100 CE for at least one of the two relative concentration pathways (RCPs) future emission scenarios. Further information on the driving global climate models (GCMs) as part of the CMIP5 can be found here: https:///verc.enes.org/data/enes-model-data/cmip5/resolution.

The future climate scenarios of the three CORDEX RCMs were analysed, taking into account the higher uncertainty on future precipitation trends in comparison to temperature trends and the interplay of changing precipitation with atmospheric warming for glacier evolution. The future climate scenarios RCP4.5 and RCP8.5 represent moderate and extreme warming by 2100 CE relative to the present day. These RCPs are often used in downscaling and climate impact studies, enabling comparison with results that used other climate or glacier model projections.Quantile mapping, also known as "distribution mapping", was used to statistically downscale the daily climate data using 14 years of observations from Pyramid and Changri Nup automatic weather stations at 5,050 and 5,600 m a.s.l (Ev-K2-CNR and GlacioClim - https://glacioclim.osug.fr/). Parametric quantile mapping (Piani et al., 2010) in particular was chosen, where a statistical relationship between the raw climate data and the observations is formed by substituting the climate model data with observations at a cumulative density function of the prescribed distribution (e.g. gaussian distribution for temperature (Luo et al., 2018); gamma for precipitation (Piani et al., 2010). This correction was then applied to the raw data to produce a third downscaled dataset which should better match the observations, though will not be identical (Maraun, et al., 2016). This approach has been found to be effective particularly for the challenging downscaling of precipitation, with errors in standard deviation, coefficient of variation and skewness of distributed values reduced relative to other methods (Lafon et al., 2012 and Reiter et al., 2018).

The observations were used to disaggregate the daily downscaled climate data to the hourly resolution required to force COSIPY, using seasonal means to reproduce the 'nocturnal peak' seen during the monsoon. The MELODIST Python tool was used for all other meteorological variables. Each of the downscaled variables from the three RCMs for the five year present day time slice was evaluated with the 14 years of observations to assess the representation of means, seasonality, diurnal cycles and day-on-day and interannual variability. In particular the representation of the monsoon was greatly improved following downscaling. The same statistical downscaling approach and disaggregation was applied to the raw CORDEX RCM daily data for the future time-slices under RCP4.5 and RCP8.5. Downscaled future climates were compared with those found in other studies using CORDEX data, finding similar annual and seasonal temperature trends for the region that are strongly linked to the RCP, and positive precipitation trends, with poor agreement between RCMs (Kaini et al., 2019 and Sanjay et al., 2017). The relationship between precipitation and RCP was less clear, showing some variation between the RCMs which may reflect the study location, with the Central Himalaya showing particularly poor RCM consensus and uncertainty in future precipitation trends with warming relative to other regions of the Hindu Kush Himalaya (Sanjay et al., 2017).

Given the absence of regional temperature projections beyond 2100 CE, global temperature change projections were applied to the end-of-century mass balances for RCP4.5 and 8.5 (Table S2). No precipitation change was applied to the post-2100 CE climate given absence of this output from the CORDEX RCMs. The glacier model was forced to 2300 CE using the downscaled RCMs mass balances calculated using the future warming scenarios RCP4.5 or RCP8.5. Minor differences in mass balance occur between the experiments used to simulate the present-day glacier; the NOAA RCM gives the best fit to observations of mass balance, and the end-of-century simulations of mass balance were less negative in the experiment using the NOAA RCM (under both RCPs) compared to the experiments using the IPSL and CCCma RCMs (Fig. S1).

Table S1. Regional Climate Models (RCMs) chosen for use in this study, and details of the Global Climate Models (GCMs) from which these are derived. The NOAA RCM that was considered most representative of conditions in the Everest region is highlighted in bold.

CORDEX South Asia regional climate model	Driving CMIPS global climate model	CMIPS modelling centre	RCM name used in this study	Future precipitation scenario	2100 CE mean temperature change from present day (℃)	
					RCP.4.5	RCP8.5
ITTM-RegCM4	NOAA-GFDL-GFDL-ESM2M	National Oceanic and Atmospheric Administration (NOAA), USA	**NOAA**	**Wet**	**1.4**	**3.8**
IITM-RegCM4	CCCma-CanESM2	Canadian Centre for Climate Modelling and Analysis (CCCma), Canada	CCCma	Moderate	2.2	4.1
IITM-RegCM4	IPSL-CMSA-LR	Institue Pierre-Simon Laplace (IPSL), France	IPSL	Dry	1.6	3.8

Table S2. Projected temperature change values for each of the RCPs in 2200 CE and 2300 CE (Collins et al., 2013)

	Temperature change from 2100 CE (°C)	
RCP	**2200 CE**	**2300 CE**
4.5	0.5	0.7
8.5	2.8	4.1

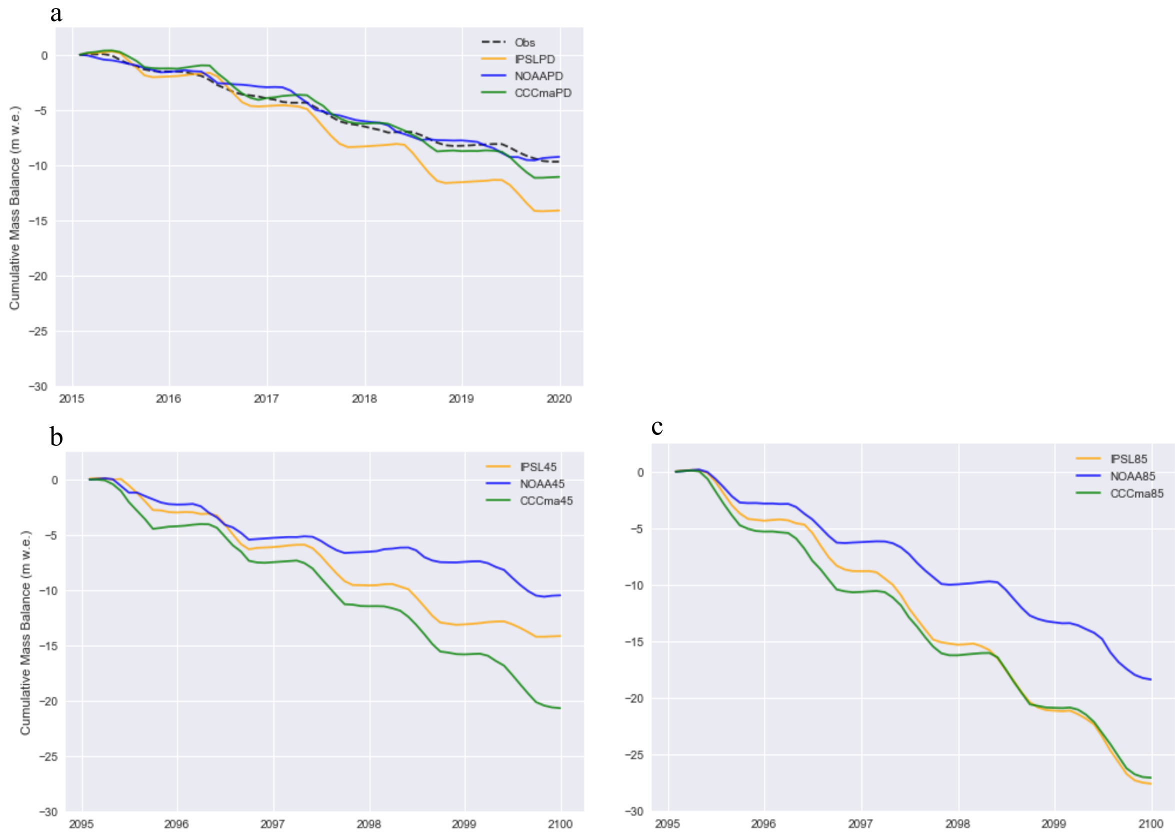

Figure S1: Spatially averaged cumulative clean-ice mass balance with clear seasonality for (a) the present day time-slice including the mass balance forced by the observations used for downscaling, and the end-of-century time-slice under (b) RCP4.5 and (c) RCP8.5. The low annual glacier-wide mass balance values shown here are the result of the extent of the model domain used to force iSOSIA that includes the larger catchment beyond the glacier margins and therefore contains a higher proportion of lower elevations than those of the glacier itself.

2. Glacier model experimental design

Khumbu Glacier is surrounded by ice-marginal moraines denoting the late Holocene (1.3 ± 0.1 ka) extent and ice thickness (Hambrey et al., 2008; Hornsey et al., 2022), which are used to constrain the historical simulations following the approach of (Rowan et al., 2015). The late Holocene glacier was reconstructed using a 5000-year equilibrium (steady state) simulation starting from an ice-free domain. The glacier at the Little Ice Age maximum was simulated by forcing the late Holocene glacier with a step change in mean annual air temperature of 1.5°C. The glacier model was then forced to the present day using each of the three distributed mass balances calculated using COSIPY and the downscaled RCMs. The distribution and rates of accumulation were improved following integration of the RCM-forced mass balances with iSOSIA, because the redistribution of snowfall by avalanching from hillslopes onto the glacier improves agreement between simulated accumulation rates and the available observations for Himalayan glaciers (Benn and Lehmkuhl, 2000). Future work to resolve the impact of low frequency–high magnitude avalanche events on accumulation rates would further refine this calculation, but the contribution of avalanches to glacier accumulation is challenging to measure.

Rock avalanching is responsible for much of the debris accumulation on the glacier surface, but there is little information about the magnitude and frequency of these events, and so debris delivery to the glacier accumulation area is assumed to be spatially and temporally uniform at a rate of 1 mm a^{-1} (Rowan et al., 2021). Debris that is incorporated into glacier ice is transported passively with ice flow following a concave path with submergence in the accumulation zone and emergence in the ablation area. If the rate of debris export from the ablation area to ice-marginal moraines is insufficient to remove debris from the glacier surface, for example during phases of net negative glacier mass balance when, then a supraglacial debris layer forms. The observed heterogeneity of ablation on the surface of Khumbu Glacier requires a parameterisation of sub-debris melt that represents the effects of differential ablation within the debris-covered area as has been previously tested for Khumbu Glacier (Rowan et al., 2021).

3. Simulated mass balance response time

The dynamic response time to a change in climatic forcing of Khumbu Glacier is expressed via an *e*-folding scale, which is defined as the time taken to complete $1–e^{-1}$ (or 63%) of the total volume change; this is preferable to calculating the time taken for glacier volume change to stabilise completely as minor volume changes often continue indefinitely. Prior to our study, the relationship between mass balance and response time had only been explored in a single study where hypothetical mass balance perturbations (–2.0 to +1.25 m water equivalent (w.e.) a^{-1} in intervals of 0.25 m w.e. a^{-1}) were applied for an equilibrium condition to Morteratsch Glacier in the Swiss Alps (Zekollari and Huybrechts, 2015). The response time of Morteratsch Glacier was 22–43 years and increased with a more positive mass balance forcing, as was also the case for Khumbu Glacier which showed a strong correlation between glacier response time and mass balance controlled by the clean-ice distributed mass balance forcing and the sub-debris ablation parameterisation (Fig. S2). This relationship between mass balance and response time occurs because strongly negative mass balance resulting from extreme warming scenarios result in acceleration in glacier volume loss, causing response times to decrease into the future as glaciers recede to higher elevations and their surfaces become steeper. A negative mass balance can increase meltwater at the glacier bed and enhance basal sliding, which would further decrease the dynamic response time. There is some evidence of this process amongst the historical Khumbu Glacier experiments, however the interplay with the impact of differing accumulation rates from the varied RCM precipitation scenarios, which also act to influence ice flux and velocities, complicate the identification of this potential coupling from our results.

4. Uncertainties associated with the glacier-climate model experimental design

The use of several RCMs to force present day and future mass balance allows the implications of climate uncertainty on glacier evolution to be simulated. The differences that stem from the RCM forcing are at times greater than those from the future RCPs due to varied predictions of future precipitation and the impact of this on glacier volume change and response time. As the CORDEX project produces only dynamically downscaled RCMs of RCP4.5 and RCP8.5 the implications of other RCPs for glacier evolution cannot be assessed. The use of a time slice mass-balance forcing approach meant that it was important to ensure that the time slices were representative of conditions for that time period and did not reflect an extreme phase of natural climate oscillation. The quantile mapping approach meant that the time-slices were the product of the 14-year calibration period. Analysis of both the temperature and precipitation trends between the present day and future time slices and the 1 km mass balance simulations of the 12 years preceding both time slices were conducted to confirm that this approach was suitable. Information on signal and variability between the present day (2015–2020 CE) and the future (2095–2100 CE) is not included in the modelling approach. An experiment was conducted using mid-century mass balance forcings to investigate the effect on glacier-climate imbalance. However this experiment produced identical results to the experiments with no mid-century forcing in 2100 CE and so was not considered necessary. The present day and end-of-century mass balances therefore put bounds on glacier evolution and so future work could address this through continuous mass balance modelling in conjunction with ice-flow modelling.

The uncertainties associated with global climate model projections increase with time after 2100 CE, particularly under RCP8.5. For example, forecasts of warming for 2281–2300 CE relative to 1986–2005 CE under RCP8.5 range from 3°C to 12.6°C (Collins et al., 2013). In the absence of results projecting changes in precipitation after 2100 CE, the precipitation was maintained at the same level for the simulations that extended beyond 2100 CE. The end-of-century precipitation amount is unlikely to be reflective of more distant future climate conditions and therefore more realistic precipitation projections are required to discover if the active glacier can be sustained further into the future or will lose mass more quickly than expected from our results. We do not expect that there will be a sufficient increase in precipitation beyond 2100 CE that could compensate for the projected warming under RCP8.5. The projected temperature changes used for the simulations of glacier evolution after 2100 CE are global averages and do not include the effects of elevation-dependent warming. Warming is likely to be higher than the global mean for the Khumbu region given that warming over land is generally at least 0.2°C higher than the global mean value applied here (Collins et al., 2013). Furthermore, higher elevations have historically warmed at faster rates than lowland regions, with warming rates up to twice that of the global mean value (Pepin et al., 2022).

Supplementary references

Biemans H., Speelman L. H., Ludwig F., Moors E., Wiltshire A., Kumar P., Gerten D., Kabat P. (2013). Future water resources for food production in five South Asian river basins and potential for adaptation – a modeling study. Science of the Total Environment. 468–469: S117–S131, doi: 10.1016/j.scitotenv.2013.05.092.

Benn DI, Lehmkuhl F. 2000. Mass balance and equilibrium-line altitudes of glaciers in high-mountain environments. Quaternary International 65–66 : 15–29. DOI: 10.1016/S1040-6182(99)00034-8

Collins, M., R. Knutti, and J. Arblaster (2013), Long-term Climate Change: Projections, Commitments and Irreversibility. In: Climate Change 2013: The Physical Science Basis. Contribution of Working Group I to the Fifth Assessment Report of the Intergovernmental Panel on Climate Change [Stocker, T.F., D. Qin, G.-K. Plattner, M. Tignor, S.K. Allen, J. Boschung, A. Nauels, Y. Xia, V. Bex and P.M. Midgley (eds.)]. Cambridge University Press, Cambridge, United Kingdom and New York, NY, USA,, 1–108.

Hambrey MJ, Quincey DJ, Glasser NF, Reynolds JM, Richardson SJ, Clemmens S. 2008. Sedimentological, geomorphological and dynamic context of debris-mantled glaciers, Mount Everest (Sagarmatha) region, Nepal. Quaternary Science Reviews 27 : 2361–2389. DOI: 10.1016/j.quascirev.2008.08.010

Hornsey J, Rowan AV, Kirkbride MP, Livingstone SJ, Fabel D, Rodes A, Quincey DJ, Hubbard B, Jomelli V. 2022. Be-10 Dating of Ice-Marginal Moraines in the Khumbu Valley, Nepal, Central

Himalaya, Reveals the Response of Monsoon-Influenced Glaciers to Holocene Climate Change. Journal of Geophysical Research: Earth Surface 127 DOI: 10.1029/2022JF006645

Kaini, S., Nepal, S., Pradhananga, S., Gardner, T. and Sharma, A. K. 2019. Representative general circulation models selection and downscaling of climate data for the transboundary Koshi river basin in China and Nepal. International Journal of Climatology, 40(9): 4131-4149. doi: 10.1002/joc.6447.

Lafon, T. et al. 2012. Bias correction of daily precipitation simulated by a regional climate model: A comparison of methods, International Journal of Climatology, 33(6): 1367–1381. doi:10.1002/joc.3518.

Li H, Sheffield J, Wood EF. 2010. Bias correction of monthly precipitation and temperature fields from Intergovernmental Panel on Climate Change AR4 models using equidistant quantile matching. Journal of Geophysical Research: Atmospheres. 115 (D10), D10101.

Luo, M. et al. (2018). Comparing bias correction methods used in downscaling precipitation and temperature from regional climate models: A case study from the Kaidu River basin in western China. Water, 10(8): 1046. doi:10.3390/w10081046.

Lutz, A., Maat, H., Biemans, H., Shrestha, A., Wester, P. and Immerzeel, W., (2016). Selecting representative climate models for climate change impact studies: an advanced envelope-based selection approach. International Journal of Climatology, 36(12): 3988-4005.

Maraun D, Wetterhall F, Ireson AM, Chandler RE. Kendon EJ, Widmann M. Brienen S. Rust H. W. Sauter T. Themeßl M. Venema V. K. C. 2010 Precipitation downscaling under climate change: recent developments to bridge the gap between dynamical models and the end user. Rev. Geophys. 48 (3), RG3003.

Pepin NC et al. 2022. Climate Changes and Their Elevational Patterns in the Mountains of the World. Reviews of Geophysics 60 DOI: 10.1029/2020RG000730

Piani, C. et al. 2010. Statistical Bias Correction of global simulated daily precipitation and temperature for the application of Hydrological Models. Journal of Hydrology, 395(3–4): 199–215. doi:10.1016/j.jhydrol.2010.10.024.

Reiter, P., Gutjahr, O., Schefczyk,L., Heinemann, G. and Casper, M. 2017. Does applying quantile mapping to subsamples improve the bias correction of daily precipitation?. International Journal of Climatology, 38(4): 1623–1633. doi:10.1002/joc.5283.

Rowan AV, Egholm DL, Quincey DJ, Glasser NF. 2015. Modelling the feedbacks between mass balance, ice flow and debris transport to predict the response to climate change of debris-covered glaciers in the Himalaya. Earth and Planetary Science Letters 430 : 427–438. DOI: 10.1016/j.epsl.2015.09.004

Rowan AV, Egholm DL, Quincey DJ, Hubbard B, King O, Miles ES, Miles KE, Hornsey J. 2021. The Role of Differential Ablation and Dynamic Detachment in Driving Accelerating Mass Loss From a Debris-Covered Himalayan Glacier. Journal of Geophysical Research: Earth Surface 126 DOI: 10.1029/2020JF005761

Sanjay, J., Krishnan, R., Shrestha, A. B., Rajbhandari, R. & Ren, G.-Y. Downscaled climate change projections for the Hindu Kush Himalayan region using CORDEX South Asia regional climate models. Advances in Climate Change Research 8, 185–198 (2017).

Zekollari H, Huybrechts P. 2015. On the climate–geometry imbalance, response time and volume–area scaling of an alpine glacier: insights from a 3-D flow model applied to Vadret da Morteratsch, Switzerland. Annals of Glaciology 56 : 51–62. DOI: 10.3189/2015AoG70A921

Zekollari, H., Huss, M. & Farinotti, D. (2019). Modelling the future evolution of glaciers in the European Alps under the EURO-CORDEX RCM ensemble. Cryosphere 13, 1125–1146.

Zekollari, H., Huss, M. and Farinotti, D. (2020). On the Imbalance and Response Time of Glaciers in the European Alps, Geophysical Research Letters, 47(2). doi: 10.1029/2019gl085578.